Chapter 6

Dissecting the steps of lymphatic metastasis

Tohru Hoshida,[1,3] Naohide Isaka,[1,3] Jeroen Hagendoorn,[1] Emmanuelle di Tomaso,[1] Bronislaw Pytowski,[2] Yen-Lin Chen,[1] Dai Fukumura,[1] Timothy P. Padera,[1] and Rakesh K. Jain.[1]

[1] E..L. Steele Laboratory for Tumor Biology, Dept. of Radiation Oncology, Massachusetts General Hospital and Harvard Medical School, Boston, MA, USA; [2] Molecular and Cellular Biology, ImClone Systems Inc., New York, NY, USA. [3] Equal contribution.

Submitted.

Abstract

Metastasis is the major cause of cancer-related death. Whereas the mechanisms for hematogenous tumor dissemination have been extensively studied, the steps leading to lymphatic metastasis have not, mainly due to a lack of appropriate animals models and imaging technologies. Here we develop a mouse model for intravital microscopy to follow tumor cell dissemination from the peritumor lymphatics of the primary tumor to the draining lymph nodes and show that the process is highly inefficient. We further show that VEGF-C increases the rate of metastasis by increasing the rate of tumor cell delivery to the lymph nodes, not by conferring a survival or growth advantage on the cells. Using a receptor-specific neutralizing monoclonal antibody we demonstrate that VEGFR-3 blockade reduces the delivery of tumor cells to the lymph node, inhibiting lymph node metastasis. VEGFR-3 blockade was not able to prevent the emergence of lymphatic metastasis in lymph nodes already seeded with tumor cells. Our new approach offers the ability to dissect the effects of relevant molecular players on individual steps of lymphatic metastasis.

Introduction

Multiple steps are required for tumor cells to metastasize from their primary site to regional lymph nodes. These steps include detachment from the primary tumor mass, invasion into lymphatic vessels, transport through draining lymphatic vessels, arrest in sentinel lymph nodes, and survival and growth in lymph nodes.[1] Each step of this process could eliminate cells from the population of potentially metastatic cells. In hematogenous metastasis each of these steps is highly inefficient, as many more cells are shed from tumors than actually form metastasis.[2] While the steps of hematogenous metastasis have been previously analyzed using intravital microscopy (IVM),[3-5] the steps in lymphatic metastasis have not been investigated due to a lack of appropriate models and imaging technologies. The inability to fully analyze the mechanisms of lymphatic metastasis has stunted the development and evaluation of therapies targeting the spread of cancer through lymphatics.

A number of experimental[6-10] and clinical studies (reviewed in[11,12]) have shown a correlation between vascular endothelial growth factor (VEGF)-C expression, tumor margin lymphangiogenesis, and lymphatic metastasis. However, the steps in the metastatic cascade that are controlled by VEGF-C are not known. VEGF-C binds to VEGFR-2, found on both blood and lymphatic vessels, and VEGFR-3, found on lymphatics vessels and some angiogenic blood vessels.[13] VEGFR-3 signaling is primarily responsible for the lymphangiogenic response to VEGF-C stimulation[14] and leads to lymphangiogenesis and lymphatic hyperplasia in mouse tumor models.[6,9,15,16] VEGF-C can also induce angiogenesis,[17,18] which can be inhibited by blocking VEGFR-2 signaling.[19] In the light of the potential clinical applications of therapies targeting VEGF-C,[8,20-22] it is important to determine the step(s) in the metastatic process regulated by VEGF-C.[23]

Here we describe an ear tumor model that allows the first intravital observation of each step in lymphatic metastasis when combined with IVM. We use these techniques to show the inefficiency in the process of lymphatic metastasis, to determine the specific step (tumor cell entry) in which VEGF-C acts to increase the rate of lymphatic metastasis, and to evaluate various therapeutic strategies for lymph node metastasis.

MATERIALS AND METHODS

Tumor cell lines. VEGF-C overexpressing (VEGF-C) and mock-transduced (MT) B16F10 melanoma and T241 fibrosarcoma cell lines were established previously and cultured as reported.[19] To create GFP-expressing cells, peak12 EF1α-GFP vector (a gift from Dr. Brian Seed) was transduced into T241-VEGF-C and T241-MT cells by lipofection. All cell lines were maintained with DMEM medium with 10% FBS. Stable expression of VEGF-C by these cell lines was verified by Northern blot analysis on total RNAs extracted from cultured cells (Supplementary Figure S1a). Western blot analysis was also carried out to confirm the secretion of VEGF-C protein (Supplementary Figure S1b). RT-PCR was carried out to demonstrate that VEGFR-2 and VEGFR-3 were not expressed by the VEGF-C overexpressing or MT tumor cells (Supplementary Figure S3a). In vitro proliferation of T241-VEGF-C, T241-MT, T241-VEGF-C-GFP, and T241-MT-GFP cells was determined by an MTT assay (Supplementary Figure S3b,c).

Animal model. Experiments were performed in nude and C57/BL6 mice and were approved by the Institutional Animal Care and Use Committee of Massachusetts General Hospital. Animals were anesthetized with ketamine/xylazine (10/100 mg/kg, i.m.) for all experiments. Lymphangiographies were performed by slow injection in the interstitial tissue of the peripheral ear and angiographies were performed by intravenous injection in the tail vein. In preliminary experiments, lymphangiography with Evan's blue dye (Sigma Chemical Co., St. Louis, MO) and FITC-dextran (2.5%, MW = 2 million; Sigma) revealed a dense auricular network of lymphatic capillaries, draining to a larger vessel at the ear base and subsequently to the exposed superficial cervical lymph node. For tumor establishment, we injected 50 μl of tumor cell suspension from excised tumors (containing $5x10^6$ cells) in the peripheral ear.

Lymphangiography by Multiphoton Laser Scanning Microscopy. Diameter of lymphatics was determined with ear lymphangiography in mice bearing T241-MT or T241-VEGF-C ear tumors, or mice without tumors. When tumor volumes reached 150 mm^3, mice were anesthetized and immobilized on a small plate with the ear fixed. 2 μl of FITC-dextran was injected in the surface of the tumors. Ear lymphatics were observed with epifluorescence intravital microscopy (IVM) and multiphoton laser scanning microscopy (MPLSM). Lymphangiography images were captured and lymphatic diameters were measured using Image J software.[9] The longest diameter of each lymphangion (a segment of lymphatics between two valves) was measured. Lymphatics within 700 μm from the edge of the tumors were defined as peritumor lymphatics and farther ones as ear base lymphatics. The afferent lymphatics to the cervical lymph node were observed in the exposed lateral neck area.

Lymph flow measurements using fluorescence photobleaching. Lymph fluid velocity in peritumor lymphatics was measured with fluorescence photobleaching as previously described.[24] Briefly, lymphangiography with FITC-dextran was performed at a constant pressure of 10 cm H_2O and the measurements were initiated when sufficient fluorescent material appeared in the lymphatics. Lymph fluid velocity was calculated by tracking the convective movement of the photobleached spot. Flow volume was calculated from the velocity and the lymphatic diameter.

Tumor cell delivery to the lymph node. Tumor cell delivery in the exposed cervical lymph node was observed with MPLSM[25,26] on day 10, 14, and 20 after tumor implantation in nude mice. No tumor cells were observed in the lymph nodes immediately after tumor implantation. To detect the lymph node capsule, collagen I was imaged using second harmonic generation[27] (Fig. 3D). T241-GFP cells or T241-VEGF-C-GFP cells were implanted in the same manner as described above. At day 10, 14 or 20, mice were anesthetized and fixed on a plate. Following tetramethylrhodamine (TMR)-dextran (1%, MW = 2 million; Molecular Probe) injection at the tip of the ear, the cervical lymph node was exposed and observed with MPLSM. Images of all the GFP positive cells detectable in our system were captured as image stacks with a 10 μm step. 1-5 fields per lymph node, 10-51 slices per stack were acquired. Numbers of cells were counted using ImageJ software in a blinded fashion by three investigators.

Direct tumor cell injection into lymph nodes. Anesthetized Mice were fixed under a stereoscope and the cervical lymph node was exposed. $1x10^3$, $5x10^3$ or $1x10^4$ of either T241-MT-GFP or T241-VEGF-C-GFP cells in 0.5 □l of PBS were directly injected into the lymph node using a 30G needle connected to a 2.5 μl microsyringe (Hamilton, Nevada) and the surgical site closed. After 28 days, lymph node tumor formation was examined macroscopically and microscopically using multiple frozen sections. ($1x10^3$ cells and $5x10^3$cells, n = 8; $1x10^4$ cells, n = 10-12)

Histological analysis. For the metastasis assay, fixed and paraffin embedded cervical lymph nodes were stained with hematoxylin and eosin. Multiple sections spaced 200 μm apart were examined. For blood and lymphatic vessel evaluation in primary tumors, ears were excised at day 14, fixed in 4% paraformaldehyde, embedded in paraffin and immunostained with rabbit anti-mouse LYVE-1-antibody (1:2000, Upstate) or MECA-32 antibody (1:50, Pharmingen). For TUNEL and Ki-67 staining, lymph nodes containing 100-500 GFP-expressing tumor cells

(determined with MPLSM as described above) were excised, fixed in 4% paraformaldehyde and frozen in OCT compound. Multiple sections were made from each sample. Fluorescent TUNEL staining was carried out according to the manufacturer's manual of ApopTag Red In Situ Apoptosis Detection Kit (Chemicon, Temecula, CA). For Ki-67 staining, sections were applied with rat anti-mouse Ki-67 antibody (Dako, Denmark) and stained with Alexa fluor 546 (Molecular probe, The Netherlands). Images were captured by confocal microscopy. The number of GFP positive/TUNEL positive cells and GFP-positive/Ki-67 positive cells were counted by two investigators in a blinded manner using Image J software. LYVE-1 staining was performed on lymph nodes containing 100-500 metastatic tumor cells prepared in the way described above. Sections were stained with rabbit anti-mouse LYVE-1 antibody (Upstate, New York) and developed with DAB. Lymphatics visualized in brightfield images were outlined and the ratio of stained lymphatic area per tissue area was analyzed with the use of an NIH image macro; n = 6-9.

Anti-VEGFR-3 antibody treatment. Rat monoclonal antibody to murine VEGFR-3, mF4 31C1 (ImClone, New York, NY)[22] was administered to mice bearing T241-VEGF-C-GFP ear tumors using different treatment schedules. To study the effect on tumor cell arrival and metastasis prevention, mF4-31C1 (40 mg/kg) was injected intraperitoneally every 2 days for the first 14 days after tumor implantation with a preload of 80 mg/kg on day 0. Rat IgG (Jackson ImmunoResearch, West Grove, PA) was injected in control mice at the same dose and schedule. Lymphatic diameter was measured with IVM lymphangiography on day12 and cell arrival into lymph nodes was quantified with MPLSM on day14 as described above. To study the ability of mF4-31C1 treatment to prevent lymph node metastasis, tumors were removed after 14 days of treatment and the treatment discontinued. Forty-two days after original tumor implantation macroscopic and microscopic metastasis were assessed. To study the ability of mF4-31C1 treatment to control metastasis formation after tumor cell seeding, T-241-VEGF-C-GFP tumors were left untreated for 14 days after implantation. On day 14, the tumors were resected and mF4-31C1 (40 mg/kg) was injected intraperitoneally every 2 days for the next 28 days with a preload of 80 mg/kg for the first dose. Forty-two days after original tumor implantation macroscopic and microscopic metastasis were assessed.

Statistics. Quantitative data are expressed and graphed as the mean ± SEM. Student's t test and Fisher's exact test were used for statistical analysis. For MTT assay results, regression analysis was used to compare slopes of graphs. Values of $p \leq 0.05$ were considered significant.

Results

Visualization of the steps of lymphatic metastasis. Using Evan's Blue or fluorescence lymphangiography accompanied by IVM and MPLSM,[25,26,28] we visualized the auricular lymphatic network draining the tip of a normal mouse ear into a larger vessel at the ear base (Nagy et al.[29]) and subsequently into the afferent lymphatic vessel of the superficial cervical lymph node (referred to as "afferent lymphatic" throughout text) (Fig. 1A-C). When tumors were implanted in the tip of the ear, each of these sets of vessels could be monitored during the metastatic process (Fig. 1D-F). We also imaged the blood vasculature of both normal and tumor bearing ears by performing simultaneous angiographies and lymphangiographies (Fig. 1G-H).

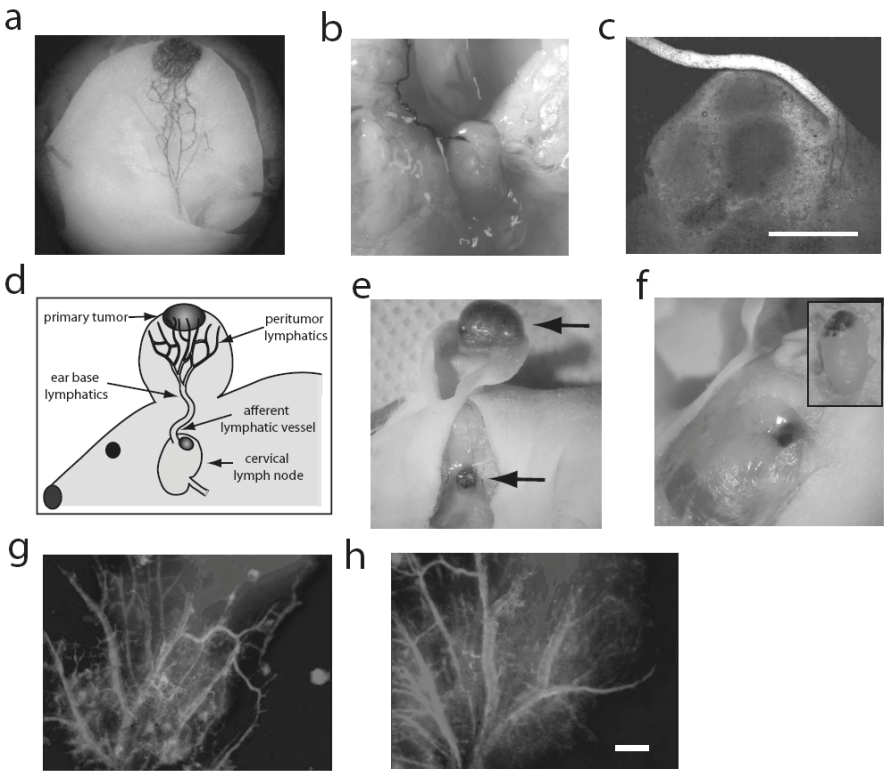

Fig. 1. Ear tumor model of lymphatic metastasis. (**A**) Evan's blue lymphangiography of normal lymphatic vessels in the mouse ear shows a network of vessels that converge into collecting lymphatics at the base of the ear. The dark blue spot at the ear-tip shows the site of dye injection. (**B**) Lymph from the ear drains into an afferent lymphatic vessel (blue) that carries lymph to the superficial cervical lymph node. (**C**) Intravital fluorescence microscopy shows the afferent lymphatic vessels draining into the cervical lymph node after fluorescence lymphangiography. Scale bar = 500 μm. (**D**) Schematic of ear tumor model showing the peritumor lymphatics, the lymphatic of the ear base and the afferent lymphatic vessel of the cervical lymph node. (**E**) A B16F10-VEGF-C tumor is grown in the tip of the ear (top arrow). A metastasis can be seen in the cervical lymph node (bottom arrow). (**F**) A metastasis from a B16F10-VEGF-C tumor forms at the junction of the afferent lymphatic vessel with the lymph node, where lymph and cells enter the node. (Inset) Excised lymph node showing a metastasis from a B16F10-VEGF-C in the tip of the node where the afferent lymphatic vessel enters.(**G,H**) Combination of angiographpy and lymphangiography in the ear. FITC (4%, 0.1 ml) was injected i.v. and TMR (1%, 2 ml) was injected at the tip of the ear or in the surface of the tumor. Images were obtained with fluorescent intravital microscopy. Top; tip of the ear, bottom; neck of the ear. Scale bar = 1 mm. (**G**) Normal vasculature (green) and lymphatic network (red), which is emerging from the tip of the ear and converging towards the neck of the ear, were observed in a normal ear. (**H**) Both peritumor blood and lymphatics vasculatures were observed in an ear with T241-VEGF-C-GFP tumor grown at the tip. Note that lymphatic and blood vessels were dilated. **(see color images)**

We next utilized our technologies to determine at which step(s) in the metastatic process VEGF-C increases the formation of lymph node metastasis. We created VEGF-C overexpressing cell lines from murine T241 fibrosarcoma and murine B16F10 melanoma[9] (Supplementary Fig. S1A-B). When implanted in the ear, VEGF-C overexpressing tumors exhibited an increased rate of lymphatic metastasis to the cervical lymph node (Supplementary Fig. S1C), without affecting the growth of the primary tumor.

Peritumor lymphatic morphology and function. Using IVM and intravital MPLSM we demonstrated that peritumor lymphatics had an increased vessel diameter around VEGF-C overexpressing T241 tumors (T241-VEGF-C) in this new tumor model when compared to mock transduced controls (T241-MT) (Fig. 2A-B). These data are consistent with our previous report using two different models.[9] Additionally, we found that the lymphatic hyperplasia extended down to the base of the ear, but was not observed in the afferent lymphatic. Consistent with this, there was no increase in density of LYVE-1 staining in the draining lymph nodes of VEGF-C overexpressing tumors compared to controls (Fig. 2C), suggesting that VEGF-C overexpression by the primary tumor did not induce lymph node lymphangiogenesis in the draining lymph node in this model.[30] Occasionally, malformed intraluminal valves were observed in the peritumor lymphatics (Supplementary Fig. S2A,B), that may contribute to abnormal flow patterns that were previously observed in these vessels.[16] LYVE-1 staining also showed enlarged tumor margin lymphatic vessels in T241-VEGF-C tumors when compared to T241-MT tumors (Fig. 2D, Supplementary Fig. S2C,D). Thus, VEGF-C induced enlargement of peritumor lymphatics provides the opportunity for increased entry of tumor cells into the lymphatic system.

Intralymphatic flow, which delivers cells to the lymph node, may also be modulated by VEGF-C. To address this possibility, we measured lymph velocity in tumor margin, ear base, and afferent lymphatic vessels with fluorescence photobleaching.[24] Although lymph velocity was lower in the peritumor lymphatics and in the lymphatics of the base of the ear in T241-VEGF-C overexpressing tumors, total flow in the lymphatics of the base of the ear was increased by 40% due to the enlarged vessel diameters (Figure 2E). Thus, the total lymph flow is significantly increased by VEGF-C overexpression, enhancing tumor cell delivery to lymph nodes.

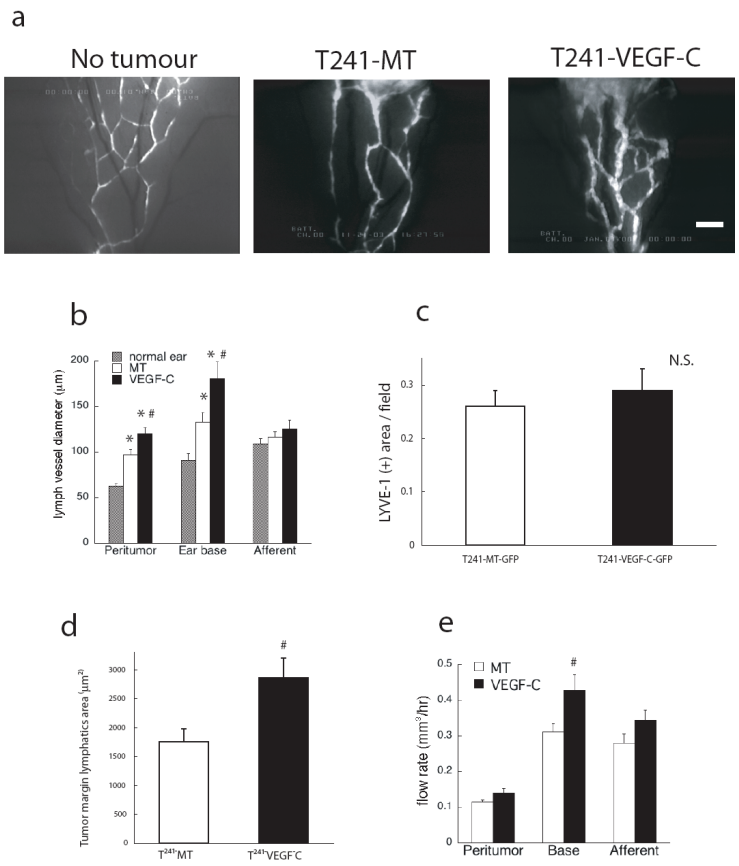

Fig. 2. Overexpression of VEGF-C induces hyperplasia of peri-tumor lymphatics and increases lymph flow rate. (**A**) Lymphangiography of peritumor lymphatics around T-241-MT and T-241-VEGF-C tumors and the equivalent vessels in a non-tumor bearing ear. Scale bar = 1 mm. (**B**) Average lymphatic vessel diameter associated with T241-VEGF-C tumors was significantly enlarged compared to T241-MT tumors and normal ears (n = 9-10) both in the peritumor area (within 700 µm from the tumor border) and the ear base area (further than 700 µm). No significant difference was observed in afferent lymphatic vessels. * indicates $p < 0.05$ when compared to normal ear; # indicates $p < 0.05$ when compared to ear bearing MT tumor. (**C**) LYVE-1 immunohistochemistry of lymph nodes draining VEGF-C overexpressing or control tumors showed no difference in lymphatic vessel density. (**D**) LYVE-1 immunohistochemistry showed that the average area of tumor margin lymphatics (within 100 µm from the tumor border) in VEGF-C overexpressing tumors (n = 129 vessels) was significantly larger than in T-241-MT tumors (n = 61 vessels). # indicates $p < 0.05$ when compared to ear bearing T-241-MT tumor. (**E**) Flow rate of ear base lymphatic vessels was significantly increased in VEGF-C overexpressing tumors (n = 8). # indicates $p < 0.05$ when compared to ear bearing MT tumor.

Intralymphatic transport of tumor cells. To image the transport of tumor cells through lymphatic vessels and into lymph nodes, we stably expressed green fluorescent protein (GFP) in T241-VEGF-C and T241-MT cells. Using MPLSM, we imaged GFP-expressing cells shed from primary tumors as they traveled in the peritumor and afferent lymphatics (Fig. 3A) and subsequently localized in the subcapsular sinus and the cortex of the lymph node near the afferent lymphatic (Fig. 3B-F). The structural collagen elements of the lymph node were imaged using second harmonic generation microscopy in order to define the location of the cells in the lymph node (Fig. 3D). The cells in the lymphatic vessels are carried by the lymph fluid to their destination, making their transport dependent on lymph flow.

VEGF-C overexpression increases tumor cell delivery to lymph nodes. An increase in lymph flow and tumor cell entry into lymphatics by VEGF-C could

increase the delivery of metastatic tumor cells to the lymph node. Using MPLSM to quantify the number of cells delivered to the lymph node revealed a significant increase in GFP-positive tumor cells in the lymph node from tumors overexpressing VEGF-C when compared to control (Fig. 3G). Twenty days after implantation, 6 out of 7 lymph nodes from mice bearing T-241-VEGF-C-GFP tumors had large metastatic nodules, whereas 8 out of 9 lymph nodes in mice bearing T-241-MT-GFP tumors had only a few tumor cells (Fig. 3E,F).

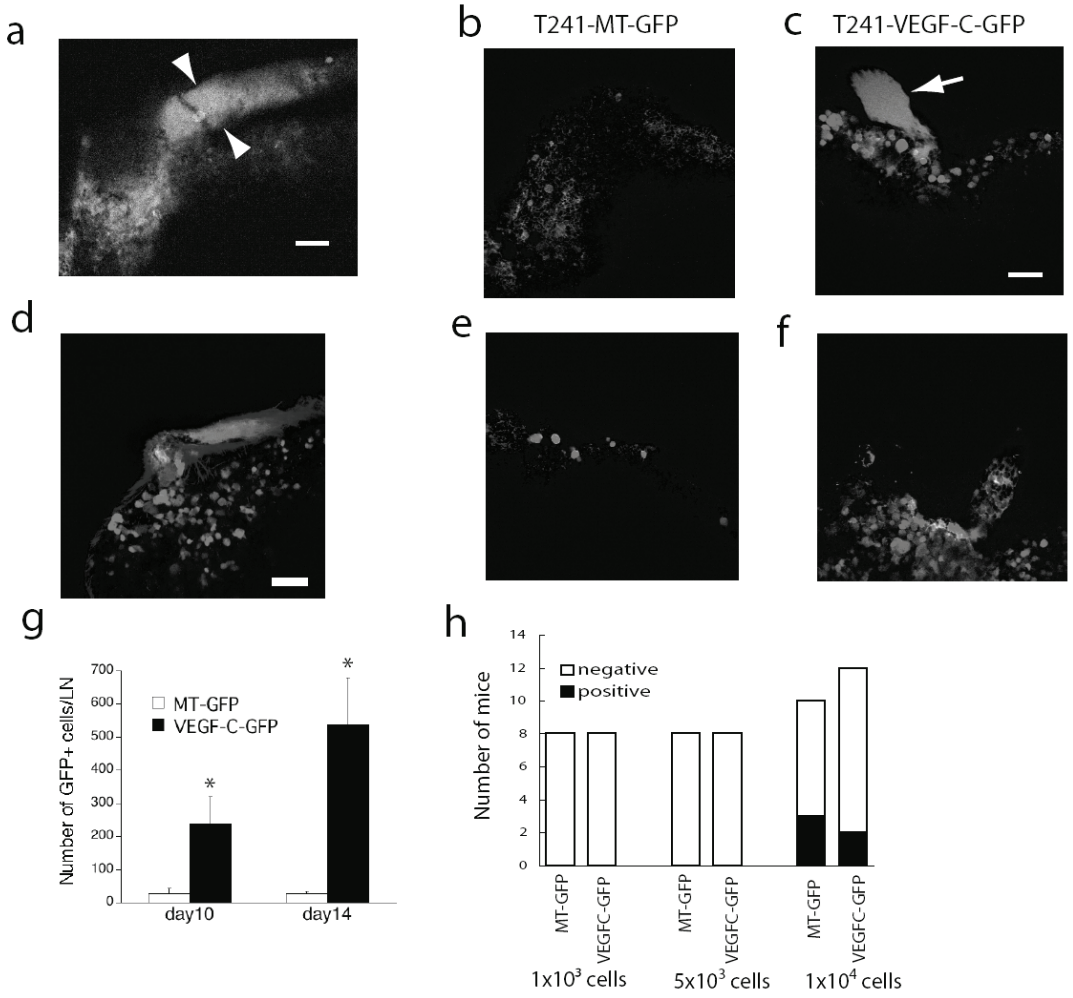

Fig. 3. Increased number of tumor cells shed from VEGF-C overexpressing tumors in the cervical lymph node imaged with MPLSM. (**A**) GFP+ tumor cell (green) in a lymphatics vessel (arrowheads) (red; TMR lymphangiography) traveling from the primary tumor to the cervical lymph node. (**B**) T-241-MT-GFP cells and (**C**) T-241-VEGF-C-GFP were observed entering the lymph node from the afferent lymphatic at day 10. Arrows denotes the afferent lymphatic vessel. Scale bar = 100 µm. (**D**) Using second harmonic generation microscopy, the collagen (blue) in the capsule of the lymph node can be detected. (**E**) At day20, 8 out of 9 lymph nodes from mice bearing T-241-MT-GFP tumors had only a few tumor cells, (**F**) whereas in mice bearing T-241-VEGF-C-GFP tumors, 6 out of 7 lymph nodes had large metastatic nodules. (**G**) A greater number of GFP-positive tumor cells arrived in the cervical lymph node from T-241-VEGF-C tumors compared to T-241-MT-GFP tumors (n = 6-7). * indicates $p < 0.05$ when compared to ear bearing T-241-MT-GFP tumor. (**H**) Direct cell injection of tumor cells into lymph nodes showed that no tumor formation occurred if less than 1×10^4 cells were injected. Tumor formation was not different between T-241-VEGF-C-GFP and T-241-MT-GFP tumor cells when 1×10^4 cells were injected into the lymph node. **(see color images)**

An alternative explanation for the increased number of T241-VEGF-C-GFP cells in the cervical lymph nodes could be that VEGF-C promotes proliferation and survival of tumor cells within the lymph nodes. However, VEGFR-2 and VEGFR-3 mRNA are not expressed in the VEGF-C overexpressing and mock-transduced (control) tumor cells and *in vitro* proliferation is not different between the cells lines (Supplementary Fig. S3A-C). We have shown previously that these VEGF-C over-expressing cells do not show increased cell migration[9]. VEGF-C overexpression did not change the rate of apoptosis or proliferation in intranodal tumor cells when compared to MT cells (Supplementary Figure S3D,E).

To specifically evaluate any role of VEGF-C overexpression in cell growth and survival in the lymph node, we developed a new technique to directly inject known numbers of tumor cells into a lymph node. By injecting equal numbers of viable T241-VEGF-C-GFP of T241-MT-GFP cells directly into the lymph node, we showed no differences in the incidence or size of tumor masses in the injected lymph nodes (Fig. 3H). Taken together, our data show VEGF-C overexpressing tumor cells have an increased delivery to the lymph node, without conferring a migratory, proliferative, or survival advantage.

Inefficiency of lymphatic metastasis. By directly injecting viable tumor cells into lymph nodes, we also noted that metastasis formation depended on the number of tumor cells injected (Fig. 3H). These data suggest that not every tumor cell that arrives in the lymph node will grow into metastatic nodules. This concept is supported by our quantification of tumor cells in the lymph nodes. 14 days after implantation of T241-MT-GFP tumor cells, an average of 27±7 tumor cells were imaged in the cervical lymph node. In T241-MT-GFP bearing animals, whose ear tumors are resected at day 14, only 1 out of 6 mice developed lymph node metastasis (Supplementary Fig. S1C). Thus, there is a level of inefficiency, similar to hematogenous metastasis,[2] in lymphatic metastasis.

Our data also suggest that the formation of metastasis from shed tumor cells is a stochastic process. Since growth and survival of VEGF-C overexpressing cells in the lymph node is the same as the control cells, the increased incidence of metastasis from T241-VEGF-C-GFP tumors is explained by increased numbers of cells arriving in the lymph node. The greater number of cells delivered to the lymph node increases the probability that a cell capable of forming a metastatic nodule will be present and form

a metastasis. The increased delivery of tumor cells may explain the correlation between VEGF-C expression and the incidence of lymph node metastasis in the clinical literature.[11,12]

VEGFR-3 blockade reduces peritumor lymphatic hyperplasia and tumor cells delivery to the lymph node. We next used our model to dissect how molecular interventions would alter the individual steps in lymphatic metastasis. We hypothesized that VEGFR-3 blockade could suppress VEGF-C induced lymphatic hyperplasia and tumor cell delivery in the lymph node. To this end, we administered a neutralizing rat monoclonal antibody to murine VEGFR-3, mF4-31C1,[22] to mice

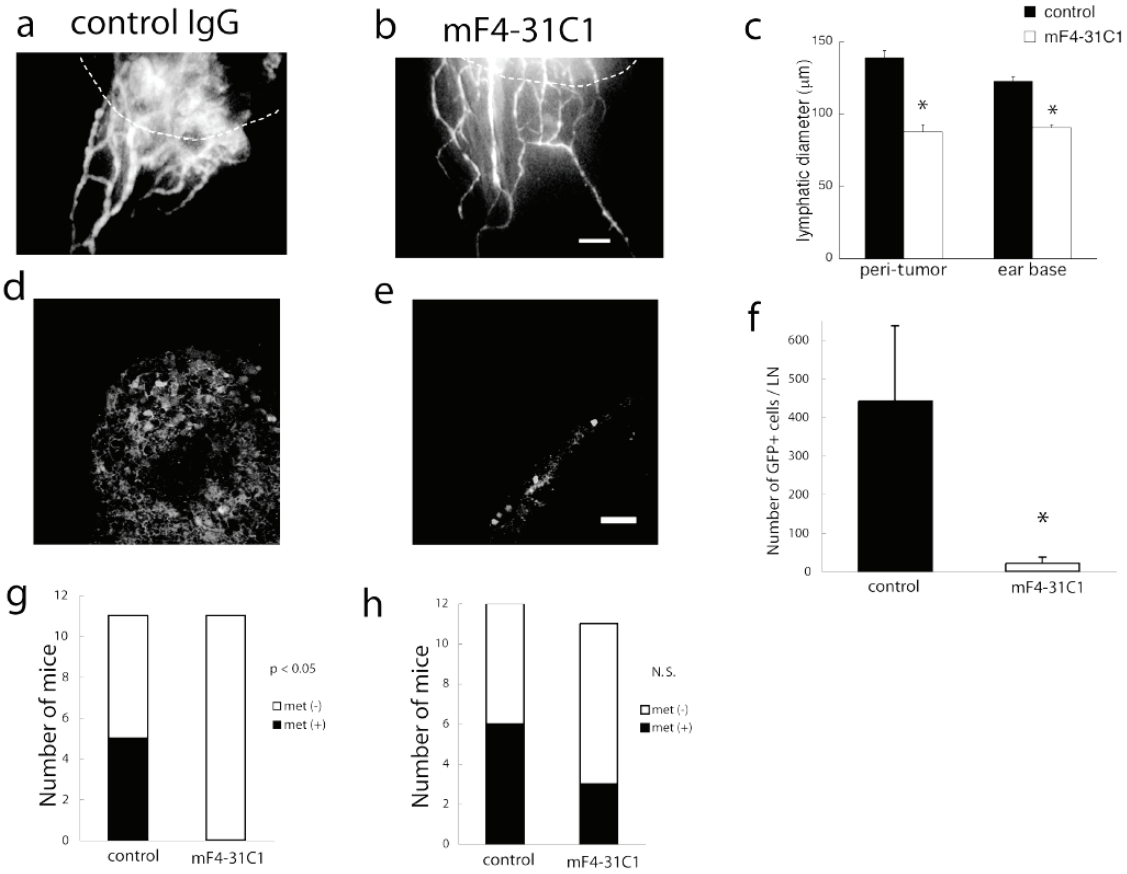

Fig. 4. Anti-VEGFR-3 antibody suppressed VEGF-C induced lymphatic hyperplasia and tumor cell arrival in the lymph nodes. (**A-C**) Peritumor and ear base lymphatic hyperplasia in VEGF-C overexpressing tumors at day12 was suppressed by every other day i.p. administration of anti-VEGFR-3 antibody (n = 8-9). White dashed line denotes tumor edge. Scale bar = 1 mm; * indicates $p < 0.05$ when compared to control IgG treated animals. (**D-F**) Number of GFP+ VEGF-C overexpressing cells in the lymph node at day 12 was significantly reduced by anti-VEGFR-3 antibody treatment (n = 8-9). (**G**) Lymph node metastasis was prevented in mice treated with mF4-31C1 from the time of tumor implantation until tumor resection at which time treatment was stopped. (**H**) Mice that had no treatment during tumor development and cell seeding of the cervical lymph node and commenced treatment with mF4-31C1 after tumor resection had gross lymph node metastasis develop. Red; TMR-dextran lymphangiography. Scale bar = 100 μm; * indicates $p < 0.05$ when compared to control IgG treated animals.

starting on the day of implantation of T241-VEGF-C-GFP tumor cells into the ear. Fluorescence lymphangiography showed that VEGF-C induced lymphatic hyperplasia was significantly suppressed by mF4-31C1 (Fig. 4A-C). This antibody did not affect intratumor blood vessel density (control 58±9 vessels/mm^2; mF4-31C1 51±7 vessels/mm^2; $p>0.05$). Furthermore, a significant decrease in the number of tumor cells delivered to the cervical lymph node of mF4-31C1 treated mice was measured on day 14 (Fig. 4D-F). VEGFR-3 blockade, however, was not able to reverse the abnormal lymph flow patterns observed in the peritumor lymphatics of VEGF-C overexpressing B16-F10 melanoma tumors implanted in the dorsal skinfold chamber (data not shown).[16]

Finally, we developed models to study the effects of different clinical situations on the ability to interfere with the process of lymphatic metastasis. To this end, we compared the development of lymph node metastasis in two different administration protocols – prevention and intervention- of mF4-31C1. In the prevention protocol, mF4-31C1 was administered from the day of T-241-VEGF-C-GFP tumor implantation until tumor resection on day 14. Consistent with the cell delivery results, fewer lymph node metastases were identified 28 days after tumor resection in the group treated with mF4-31C1 (Fig. 4G). In the intervention protocol, T-241-VEGF-C-GFP tumors were left untreated for 14 days and then resected. Treatment with mF4-31C1 was started and continued for 28 days. No statistical difference in lymph node metastasis was found between control and mF4-31C1 treated animals (Figure 4H). Although VEGFR-3 blockade successfully blocked lymphatic hyperplasia and limited the delivery of tumor cells into the lymph node, it was unable to prevent the growth of seeded tumor cells in each lymph node. These studies are critically important for guiding the use of similar lymphatic targeted therapies in the clinic.

Discussion

The model that we developed is ideally suited to dissect the individual steps in lymphatic metastasis using non-invasive intravital microscopy. It is the first model that allows in vivo assessment of peritumor lymphatic function, lymphangiogenesis and angiogenesis, and tumor cell delivery to the lymph node in the same animal.

Although the model is limited by the necessity of surgical exposure of the cervical lymph node for imaging, difficulties in stabilizing the lymph node preparation during imaging and a low rate of tumor formation in the ear with some tumor cell lines, it is powerful model to study the effects of lymphangiogenic growth factors and potential therapeutic agents on the process of lymphatic metastasis.

Using this model, we showed that the process of lymphatic metastasis is inefficient and have identified tumor cell entry as the step in which VEGF-C increase the rate of lymphatic metastasis (Figure 5). Thus, the increase in macroscopic lymph node metastases associated with VEGF-C expression seen in experimental and clinical studies is the result of a greater number of cells delivered to the lymph node, increasing the probability that a metastasis will form.

The exact mechanism by which VEGF-C increases tumor cell entry into lymphatic vessels is not known. One hypothesis is that VEGF-C increases the surface area of functional lymphatics in the tumor margin, thus providing more opportunity for a tumor cell to enter the lymphatics and disseminate [9]. The data presented here support this hypothesis. An alternate hypothesis is that VEGF-C stimulates tumor associated lymphatics or the draining lymph nodes to release chemotactic factors that recruit tumor cells to enter lymphatics[31-34]. Further mechanistic studies on the entry of cancer cells into lymphatic vessels can clarify whether the lymphatics only act as passive recipients of invasive tumor cells or whether they play an active role in tumor cell invasion.

Interfering in the VEGF-C/VEGFR-3 signaling pathway has been suggested as a useful clinical strategy in the treatment of lymphatic metastasis.[8,21-23] The expression of a soluble VEGFR-3 receptor, which competitively inhibits the binding of VEGF-C and VEGF-D to both VEGFR-2 and VEGFR-3, is able to prevent lymph node metastasis when the soluble receptor is available from the time of tumor implantation.[21,34,35] VEGF-C also stimulates angiogenesis through VEGFR-2 stimulation,[17-19] hence the use of the soluble VEGFR-3 receptor interferes with this mechanism. To isolate the contribution of VEGFR-3 in promoting lymphatic metastasis, we directly blocked VEGFR-3 signaling by using the neutralizing rat monoclonal antibody mF4-31C1 and demonstrate that lymphatic hyperplasia, and consequently, the number of tumor cells entering into lymphatic vessels can be reduced. The reduction of the number of tumor cells entering into lymphatic vessels significantly reduced the number of lymph node metastasis in the absence of any

direct effect of the treatment on the cancer cells. These data offer novel mechanistic insight into the correlation between VEGF-C and lymph node metastasis and demonstrate that VEGFR-3 blockade may be a valid strategy to *prevent* lymph node metastasis.

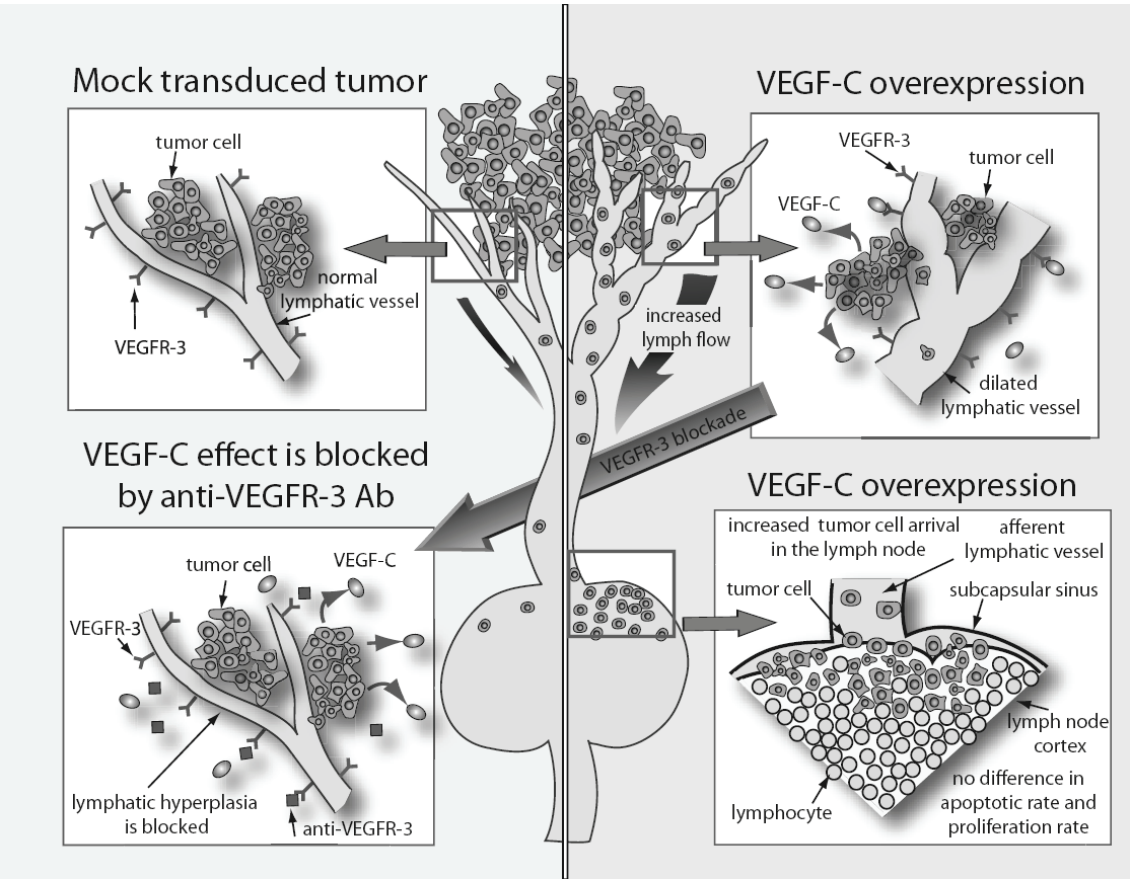

Fig. 5. Dissecting the steps in lymphatic metastasis has led to new insights into the process. VEGF-C secreted from tumor cells stimulates VEGFR-3 expressed in lymphatic endothelial cells, and thus induces hyperplasia in peritumor lymphatics (right upper panel). An increased lymphatic surface area increases the opportunity of tumor cell entry into lymphatic vessels. Augmented lymph flow also enhances tumor cell delivery to draining lymph nodes. On the other hand, mock-transduced tumors did not induce a strong lymphatic hyperplasia, although lymphatic diameter was enlarged compared to normal ears (left upper panel). An increased number of tumor cells were delivered to the cervical lymph node of mice bearing VEGF-C overexpressing tumors (right lower panel). Many more tumor cells arrive in the lymph node than go on to form metastatic tumors, highlighting the inefficiency in this process. Apoptosis and proliferation rate of tumor cells in the lymph nodes were not increased in VEGF-C overexpressing tumors. Anti-VEGFR-3 antibody treatment markedly blocked the VEGF-C induced lymphatic hyperplasia and the tumor cell delivery to lymph nodes (left lower panel). VEGF-C seems to increase lymphatic metastasis by increasing lymphatic surface area and lymph flow rate at the point of tumor cell entry into lymphatic vessels.

On the other hand, VEGFR-3 blockade was not effective in blocking metastasis formation in lymph nodes already seeded with cancer cells that do not express VEGFR-3. Although VEGFR-3 is present on some tumor blood vessels and can play

a role in tumor angiogenesis[36,37], VEGFR-3 blockade did not inhibit growth of the primary tumor, blood vessel density or metastatic growth in our model.

Dissecting the pathways of lymphatic metastasis has shown that VEGF-C/VEGFR-3 signaling acts at the site of tumor cell entry into lymphatic vessels. This information should be used to guide the selection of clinical situations in which anti-lymphatic therapy will be beneficial. Patients with disease confined to the primary site who can be successfully treated with local therapy (e.g. surgery) are unlikely to benefit from anti-lymphatic therapy. Similarly, patients with successful treatment of their primary tumor, but with tumor cells already seeded to the lymph node, may derive little benefit from anti-lymphatic therapy. In contrast, settings where the prevention of tumor cell seeding into lymphatic vessels is indicated, anti-lymphatic therapy is a very promising therapeutic strategy. Examples of such settings include patients with inoperable tumors, patients with residual cancer cells after surgical resection or those at risk of local failure after initial treatment.[12] In the specific circumstances in which the VEGFR-3 receptor is present on tumors cells or the tumor angiogenesis is dependent on VEGFR-3 signaling, VEGFR-3 blockade may have additional benefit in treating metastatic disease. The efficacy of anti-lymphatic therapy in these clinical settings now needs to be validated in clinical trials.

ACKNOWLEDGEMENTS

The authors thank Sergey Kozin, Lance Munn, and Gregory Nelson for their scientific and technical help and Sylvie Roberge, Julia Kahn, Jessica Tooredman, Nyall London, and Carolyn Smith for their outstanding technical support. This work was supported by NCI Grant #R01-CA85140.

REFERENCES

1. Fidler IJ. Critical determinants of metastasis. *Semin Cancer Biol*. 2002;12:89-96.
2. Butler TP, Gullino PM. Quantitation of cell shedding into efferent blood of mammary adenocarcinoma. *Cancer Res*. 1975;35:512-6.
3. Chambers AF, Groom AC, MacDonald IC. Dissemination and growth of cancer cells in metastatic sites. *Nat Rev Cancer*. 2002;2:563-72.
4. Condeelis J, Segall JE. Intravital imaging of cell movement in tumours. *Nat Rev Cancer*. 2003;3:921-30.
5. Kim JW, Wong CW, Goldsmith JD, Song C, Fu W, Allion MB, Herlyn M, Al-Mehdi AB, Muschel RJ. Rapid apoptosis in the pulmonary vasculature distinguishes non-metastatic from metastatic melanoma cells. *Cancer Lett*. 2004;213:203-12.
6. Skobe M, Hawighorst T, Jackson DG, Prevo R, Janes L, Velasco P, Riccardi L, Alitalo K, Claffey K, Detmar M. Induction of tumor lymphangiogenesis by VEGF-C promotes breast cancer metastasis. *Nat Med*. 2001;7:192-8.
7. Mandriota SJ, Jussila L, Jeltsch M, Compagni A, Baetens D, Prevo R, Banerji S, Huarte J, Montesano R, Jackson DG, Orci L, Alitalo K, Christofori G, Pepper MS. Vascular endothelial growth factor-C-mediated lymphangiogenesis promotes tumour metastasis. *Embo J*. 2001;20:672-82.
8. Karpanen T, Egeblad M, Karkkainen MJ, Kubo H, Yla-Herttuala S, Jaattela M, Alitalo K. Vascular endothelial growth factor C promotes tumor lymphangiogenesis and intralymphatic tumor growth. *Cancer Res*. 2001;61:1786-90.
9. Padera TP, Kadambi A, di Tomaso E, Carreira CM, Brown EB, Boucher Y, Choi NC, Mathisen D, Wain J, Mark EJ, Munn LL, Jain RK. Lymphatic metastasis in the absence of functional intratumor lymphatics. *Science*. 2002;296:1883-6.
10. Wong SY, Haack H, Crowley D, Barry M, Bronson RT, Hynes RO. Tumor-secreted vascular endothelial growth factor-C is necessary for prostate cancer lymphangiogenesis, but lymphangiogenesis is unnecessary for lymph node metastasis. *Cancer Res*. 2005;65:9789-98.
11. Nisato RE, Tille JC, Pepper MS. Lymphangiogenesis and tumor metastasis. *Thromb Haemost*. 2003;90:591-7.
12. Achen MG, McColl BK, Stacker SA. Focus on lymphangiogenesis in tumor metastasis. *Cancer Cell*. 2005;7:121-7.
13. Saharinen P, Tammela T, Karkkainen MJ, Alitalo K. Lymphatic vasculature: development, molecular regulation and role in tumor metastasis and inflammation. *Trends Immunol*. 2004;25:387-95.
14. Veikkola T, Jussila L, Makinen T, Karpanen T, Jeltsch M, Petrova TV, Kubo H, Thurston G, McDonald DM, Achen MG, Stacker SA, Alitalo K. Signalling via vascular endothelial growth factor receptor-3 is sufficient for lymphangiogenesis in transgenic mice. *Embo J*. 2001;20:1223-31.
15. He Y, Rajantie I, Ilmonen M, Makinen T, Karkkainen MJ, Haiko P, Salven P, Alitalo K. Preexisting lymphatic endothelium but not endothelial progenitor cells are essential for tumor lymphangiogenesis and lymphatic metastasis. *Cancer Res*. 2004;64:3737-40.
16. Isaka N, Padera TP, Hagendoorn J, Fukumura D, Jain RK. Peritumor lymphatics induced by vascular endothelial growth factor-C exhibit abnormal function. *Cancer Res*. 2004;64:4400-4.
17. Cao YH, Linden P, Farnebo J, Cao RH, Eriksson A, Kumar V, Qi JH, Claesson-Welsh L, Alitalo K. Vascular endothelial growth factor C induces angiogenesis in vivo. *Proceedings of the National Academy of Sciences of the United States of America*. 1998;95:14389-14394.
18. Witzenbichler B, Asahara T, Murohara T, Silver M, Spyridopoulos I, Magner M, Principe N, Kearney M, Hu JS, Isner JM. Vascular endothelial growth factor-C (VEGF-C/VEGF-2) promotes angiogenesis in the setting of tissue ischemia. *American Journal of Pathology*. 1998;153:381-394.

19. Kadambi A, Carreira CM, Yun CO, Padera TP, Dolmans DE, Carmeliet P, Fukumura D, Jain RK. Vascular endothelial growth factor (VEGF)-C differentially affects tumor vascular function and leukocyte recruitment: role of VEGF-receptor 2 and host VEGF-A. *Cancer Research*. 2001;61:2404-8.
20. Alitalo K, Mohla S, Ruoslahti E. Lymphangiogenesis and cancer: meeting report. *Cancer Res*. 2004;64:9225-9.
21. He Y, Kozaki K, Karpanen T, Koshikawa K, Yla-Herttuala S, Takahashi T, Alitalo K. Suppresion of tumor lymphangiogenesis and lymph node metastasis by blocking vascular endothelial growth factor receptor-3 signalling. *Journal of the National Cancer Institute*. 2002;94:819-825.
22. Pytowski B, Goldman J, Persaud K, Wu Y, Witte L, Hicklin DJ, Skobe M, Boardman KC, Swartz MA. Complete and specific inhibition of adult lymphatic regeneration by a novel VEGFR-3 neutralizing antibody. *J Natl Cancer Inst*. 2005;97:14-21.
23. Gershenwald JE, Fidler IJ. Cancer. Targeting lymphatic metastasis. *Science*. 2002;296:1811-2.
24. Berk DA, Swartz MA, Leu AJ, Jain RK. Transport in lymphatic capillaries. II. Microscopic velocity measurement with fluorescence photobleaching. *American Journal of Physiology*. 1996;270:H330-7.
25. Brown EB, Campbell RB, Tsuzuki Y, Xu L, Carmeliet P, Fukumura D, Jain RK. In vivo measurement of gene expression, angiogenesis and physiological function in tumors using multiphoton laser scanning microscopy. *Nature Medicine*. 2001;7:864-8.
26. Padera TP, Stoll BR, So PT, Jain RK. Conventional and high-speed intravital multiphoton laser scanning microscopy of microvasculature, lymphatics, and leukocyte-endothelial interactions. *Mol Imaging*. 2002;1:9-15.
27. Brown E, McKee T, diTomaso E, Pluen A, Seed B, Boucher Y, Jain RK. Dynamic imaging of collagen and its modulation in tumors in vivo using second-harmonic generation. *Nat Med*. 2003;9:796-800.
28. Jain RK, Munn LL, Fukumura D. Dissecting tumour pathophysiology using intravital microscopy. *Nat Rev Cancer*. 2002;2:266-76.
29. Nagy JA, Vasile E, Feng D, Sundberg C, Brown LF, Detmar MJ, Lawitts JA, Benjamin L, Tan X, Manseau EJ, Dvorak AM, Dvorak HF. Vascular permeability factor/vascular endothelial growth factor induces lymphangiogenesis as well as angiogenesis. *J Exp Med*. 2002;196:1497-506.
30. Hirakawa S, Kodama S, Kunstfeld R, Kajiya K, Brown LF, Detmar M. VEGF-A induces tumor and sentinel lymph node lymphangiogenesis and promotes lymphatic metastasis. *Journal of Experimental Medicine*. 2005;201:1089-1099.
31. Muller A, Homey B, Soto H, Ge N, Catron D, Buchanan ME, McClanahan T, Murphy E, Yuan W, Wagner SN, Barrera JL, Mohar A, Verastegui E, Zlotnik A. Involvement of chemokine receptors in breast cancer metastasis. *Nature*. 2001;410:50-6.
32. Pepper MS, Skobe M. Lymphatic endothelium: morphological, molecular and functional properties. *J Cell Biol*. 2003;163:209-13.
33. Wang W, Goswami S, Sahai E, Wyckoff JB, Segall JE, Condeelis JS. Tumor cells caught in the act of invading: their strategy for enhanced cell motility. *Trends Cell Biol*. 2005;15:138-45.
34. He Y, Rajantie I, Pajusola K, Jeltsch M, Holopainen T, Yla-Herttuala S, Harding T, Jooss K, Takahashi T, Alitalo K. Vascular endothelial cell growth factor receptor 3-mediated activation of lymphatic endothelium is crucial for tumor cell entry and spread via lymphatic vessels. *Cancer Res*. 2005;65:4739-46.
35. Lin J, Lalani AS, Harding TC, Gonzalez M, Wu WW, Luan B, Tu GH, Koprivnikar K, VanRoey MJ, He Y, Alitalo K, Jooss K. Inhibition of lymphogenous metastasis using adeno-associated virus-mediated gene transfer of a soluble VEGFR-3 decoy receptor. *Cancer Res*. 2005;65:6901-9.

36. Partanen TA, Alitalo K, Miettinen M. Lack of lymphatic vascular specificity of vascular endothelial growth factor receptor 3 in 185 vascular tumors. *Cancer*. 1999;86:2406-12.
37. Valtola R, Salven P, Heikkila P, Taipale J, Joensuu H, Rehn M, Pihlajaniemi T, Weich H, deWaal R, Alitalo K. VEGFR-3 and its ligand VEGF-C are associated with angiogenesis in breast cancer. *Am J Pathol*. 1999;154:1381-90.

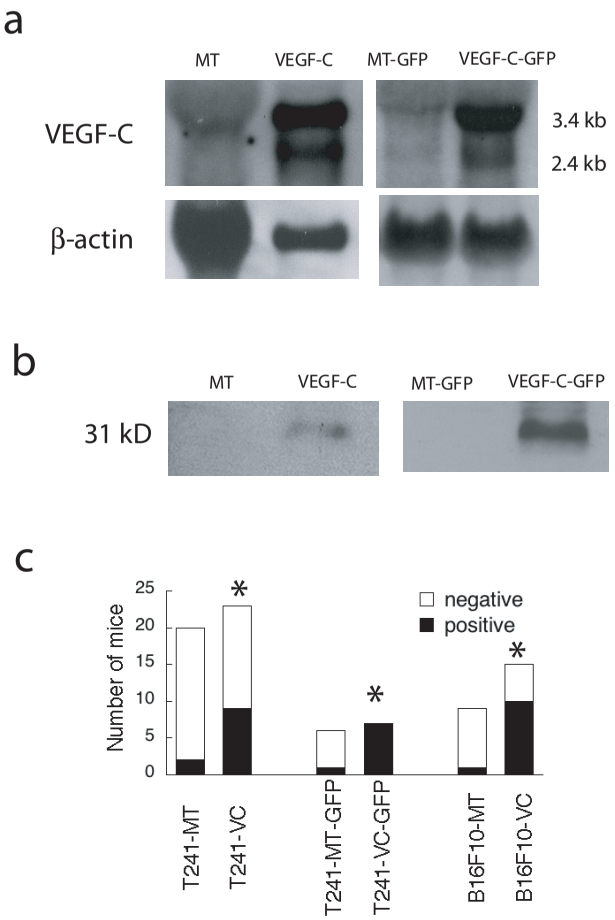

Supplementary Figure S1. (**a**) Stable expression of VEGF-C in VEGF-C transduced cell lines was verified by Northern blot analysis on total RNAs extracted from cultured cells. Two bands (3.4 kb and 2.4 kb) correspond to the full-length transcript and a splice product lacking ~1kb of viral non-long terminal regions. Rehybridization with a β-actin probe was performed as a loading control. (**b**) Western blot analysis was also carried out to confirm the secretion of VEGF-C protein, using a polyclonal anti-VEGF-C antibody (dilution, 1:000, Santa Cruz, Santa Cruz, CA). Analysis of conditioned media confirmed abundant secretion of the partially processed 31 kD form of VEGF-C in VEGF-C transduced cell lines, but not in mock transduced cell lines. (**c**) Overexpression of VEGF-C in T241 fibrosarcomas and B16F10 melanomas in the mouse ear markedly increases the rate of lymphatic metastasis to the cervical lymph node. Primary tumors were resected at day 14. * $P < 0.05$.

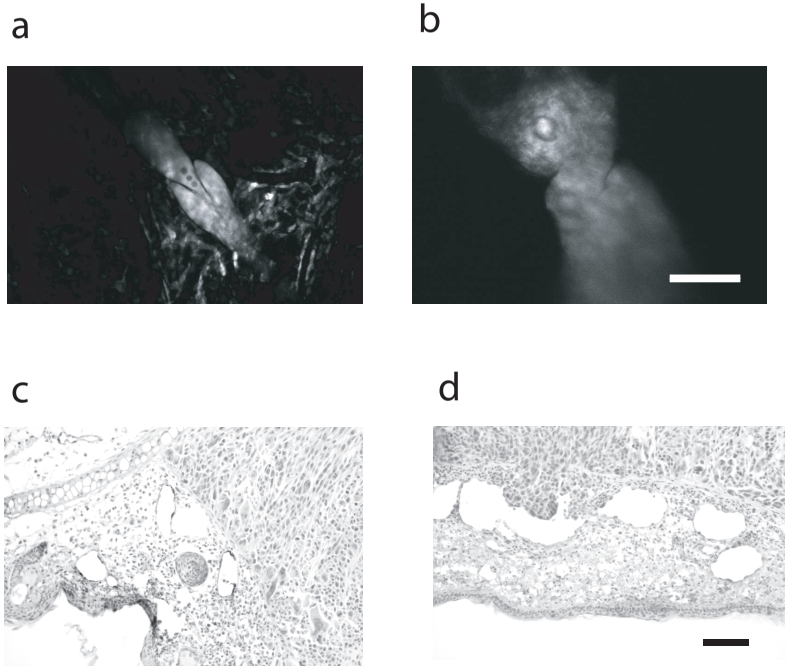

Supplementary Figure S2. Overexpression of VEGF-C induces hyperplasia of peritumor lymphatics. **(a)** Lymphatic valves were observed in peritumor lymphatics of MT tumors with MPLSM lymphangiography. **(b)** Occasionally, malformed lymphatic valves were observed in dilated peritumor lymphatics of VEGF-C overexpressing tumors. Scale bar = 100 μm **(c)** Tumor margin lymphatics in T241-MT tumors were detected with LYVE-1 lymphatic endothelial cell staining. **(d)** Enlarged lymphatics were observed in T241-VEGF-C tumors. Scale bar = 100 μm

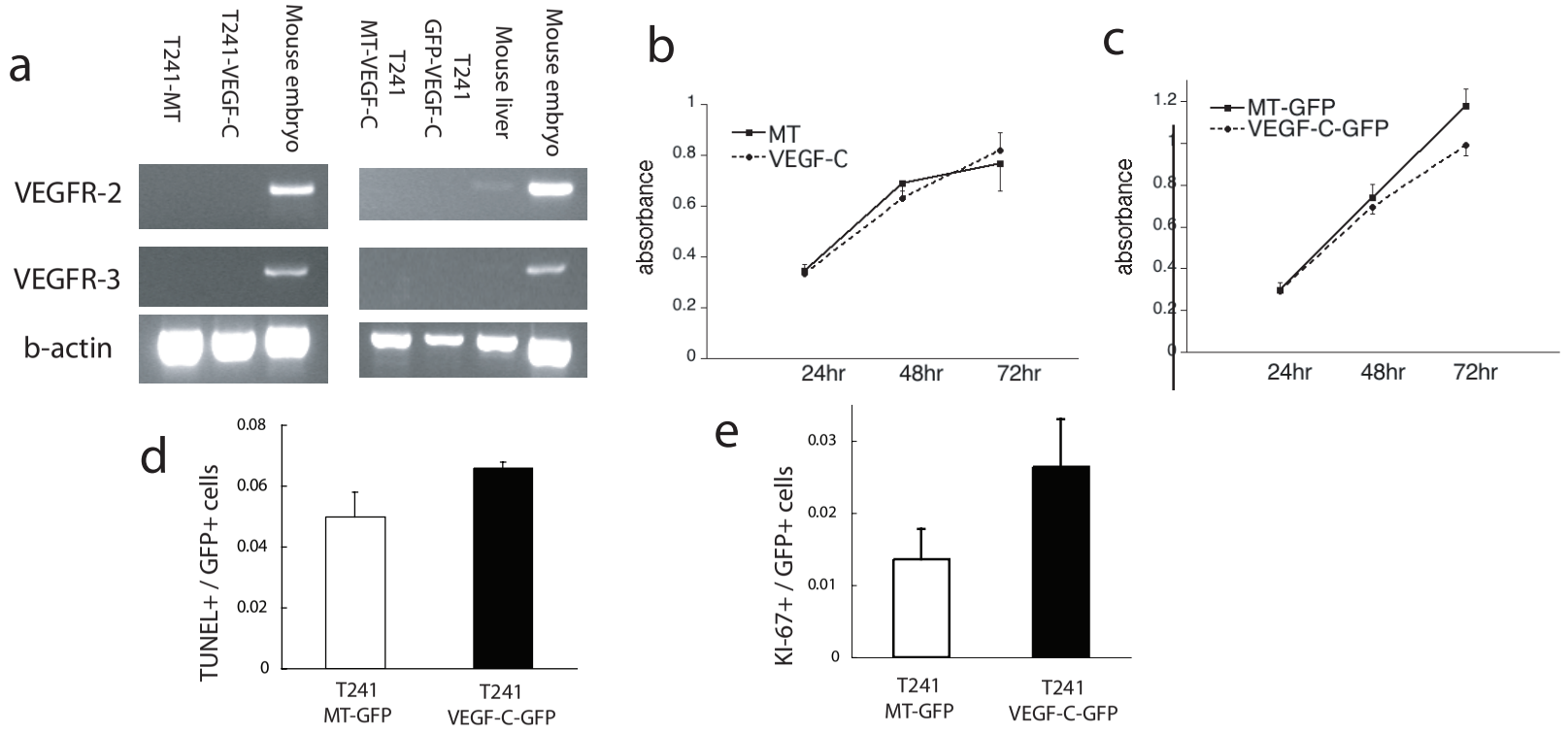

Supplementary Figure S3. **(a)** RT-PCR from cultured cells demonstrated that VEGFR-2 and VEGFR-3 mRNA were not expressed either in VEGF-C overexpressing or MT tumor cells. Total RNA was extracted from cultured cells using RNeasy kit (Qiagen, Valencia, CA) and reverse transcribed using TaqMan kit (Applied Biosystems, Foster City, CA). PCR reaction was conducted with primer pairs for VEGFR-2 and VEGFR-3 (primers: VEGFR-2 forward, 5'-GCTTTCGGTAGTGGGATGAA-3', reverse, 5'-GGAATCCATAGGCGAGATCA-3'; VEGFR-3 forward, 5'-TTGGCATCAATAAAGGCAG-3', reverse, 5'-CTGCGTGGTGTACACCTTA-3') PCR products were electrophoresed in an agarose gel and receptor gene expression was analyzed. Mouse embryo and mouse liver mRNA were used for positive control. **(b,c)** In vitro proliferation of T241-VEGF-C, T241-MT, T241-VEGF-C-GFP, and T241-MT-GFP cells was determined by an MTT assay. 3x10^3 of cells were plated on 96-well plates in triplicate. After 24, 48, or 72 hours incubation, 20 ml of MTT (2 mg/ml) was added to each well for 2-hour incubation. Then, 100 ml of DMSO was added and absorbance was measured with a multi-plate reader. All assays were performed in duplicate. **(d)** VEGF-C over-expression did not change the rate of apoptotic intranodal tumor cells (TUNEL-positive GFP-positive tumor cells; 6.6% ± 1.9%; n = 5) when compared to MT cells (5.0% ± 0.8%; n = 6; $p > 0.05$). **(e)** Similarly, VEGF-C over-expression did not change the rate of proliferating intranodal tumor cells (Ki-67-positive GFP-positive tumor cells; 2.6% ± 0.7%; n = 6) when compared to MT cells (1.4% ± 0.4%; n = 9; $p > 0.05$).